# Optimization of Calcination Temperature to Synthesis ZnO Nanostructures as Photocatalyst Using Pineapple as Chelating Agent



# Optimization of Calcination Temperature to Synthesis ZnO Nanostructures as Photocatalyst Using Pineapple as Chelating Agent

**Abrar Ismardi[1*], Indra Wahyudhin Fathona[1], Anisa Nur Rezky[1], Nor Hakimin Abdullah[2], Aurisa Prastika[1], Mukhammad Fahlevi Ali Rafsanjani[1], Siti Ashila Farikha Mayundri[1], Theresia Deviyana Gunawan[1]**

[1]Department of Engineering Physics, Telkom University, Jl. Telekomunikasi No.1 Terusan Buah Batu, Bandung, 40257, Indonesia
[2] Faculty of Bioengineering and Technology, Universiti Malaysia Kelantan Jeli Campus, Locked Bag No. 100, 17600, Jeli, Kelantan, Malaysia

Email: abrarselah@telkomuniversity.ac.id

**Abstract**. ZnO nanostructures were successfully synthesized using the sol-gel method with pineapple extract (*Ananas comosus (L.)*) as a chelating agent. ZnO nanostructures using cayenne pineapple (*Ananas comosus var.cayenne*) chelate were calcined at temperatures ranging from 500 ˚C to 900 ˚C, while queen pineapple (*Ananas comosus var.queen*) was calcined at 700 ˚C and 800 ˚C. ZnO nanostructures synthesized with cayenne pineapple chelate and calcinated at 800 ˚C showed an average particle size of 1.858 µm and an average crystallite size of 35.10 nm, while at 700 ˚C, it was 30.90 nm. The diffraction peaks can be indexed as a hexagonal wurtzite structure ($a = 3.25x10^{-10}$ m, $c = 5.21x10^{-10}$ m). The photocatalytic activity of ZnO was evaluated for the photodegradation of methylene blue under UV light radiation. The most effective degradation was achieved with ZnO nanostructures synthesized with cayenne pineapple chelate at a calcination temperature of 700 ˚C under UV light irradiation for 240 minutes. The degradation rate was 55.87% at a concentration of 10 ppm MB solution.

## 1. Introduction

Water is the most vital natural resource for humans, but water pollution caused by textile waste is a significant problem, particularly in Indonesia. In West Java Province, Indonesia, over 3000 industries dump their waste into the Citarum River, which is the primary source of water for 27.5 million people living in West Java Province and Jakarta City. It is also the primary irrigation system for more than 400 hectares of agricultural land [1]. The textile dyes used by these factories reside in the waste for about 15-20%, eventually flowing into the nearby environment, causing disturbances in the water ecosystem [2]. One of the dyes used for textile production is methylene blue, a heterocyclic aromatic chemical compound with the chemical formula $C_{16}H_{18}N_3SCl$ [3]. According to the regulation of The Ministry of Environment of Indonesia, no. Kep51/MENLH/101995, the limit for methylene blue allowed in water is 5-10 mg/L.

There are many methods used to overcome the textile waste problem. For example, using active mud [4–6] or anaerobic with bioremediation processes [7–9], the most common method is photodegradation, utilizing photocatalyst [10–12]. Nanostructures used for photocatalyst are ZnO. ZnO nanostructures are beneficial for photocatalysis since Zn has a lower negative standard reduction potential compared to any

other metal; for example, Fe reduction power is weaker than Zn [13]. Because the reduction power of Zn is more powerful, the degradation rate of Zn contaminant is faster than Fe. The other advantage of using ZnO is, it is possible to capture energy from a wider spectrum of sun than other semiconductor metal, like $SnO_2$ and $TiO_2$.

The synthesis of ZnO nanostructures can be accomplished through various methods, including sol-gel [14–16], hydrothermal [17,18], precipitation [19,20], solvothermal [21,22], microemulsion [23,24], electrochemical deposition [25,26], microwave [27,28], polyol [29,30], flux method [31], electrospinning [32,33], and wet chemical methods [34,35]. Among these methods, sol-gel is considered an inexpensive and effective technique for synthesizing ZnO nanostructures due to its ability to provide good homogeneity, high purity, energy efficiency, low pollution, and a fast crystallization and separation phase [36]. In the process of synthesizing ZnO nanostructures using the sol-gel method, a chelating agent such as Zinc acetate is typically used to reduce clotting or agglomeration [37].

In previous research by D. Štrbac et al. (2018), it was proven that methylene blue dye could be successfully degraded using ZnO as a photocatalyst [12]. Ahmad et al. carried out the bio-synthesis of ZnO nanoparticles using pineapple extract, and the results showed that the particle size of the ZnO nanoparticles ranged from 30 to 57 nm. These nanoparticles were then used for E. coli antibacterial removal [38]. However, some papers have not reported the effect of calcination temperature on nanostructure synthesis. Temperature is an important synthesis parameter and a sensitive issue, and it is the main focus of this research.

This research focuses on the green synthesis of ZnO nanostructures and studies the effect of calcination temperature and the usage of different types of chelating agents from pineapple, which are *Ananas comosus var. Queen* and *Ananas comosus var. cayenne*. It is hoped that this study will provide an optimum calcination temperature and type of chelating agent to synthesize ZnO nanostructures. Meanwhile, the degradation process of methylene blue using ZnO nanostructures can be done more efficiently, and of course the sample will be environmentally friendly since it was made with green synthesis.

## 2. Material and Methods

### *2.1. Preparation of Pineapple extracts*

Pineapple extracts play a major role in this experiment as chelating agents since they contain 78% citric acid and have a high sugar level. The pineapple was extracted by mashing the fruit into a smooth substrate. The residue was then separated from the extract using filter paper. The chelating agent was used to prevent agglomeration during nanostructure synthesis.

### *2.2. Synthesis of ZnO Nanostructures using Pineapple extracts*

ZnO particles were mixed with 100 ml of HCl in a beaker glass and then heated using a hotplate magnetic stirring at 90 °C and 200 rpm for 5 minutes. A chelating agent with a volume of 210 ml was then added to the beaker glass and heated again at 90 °C until the solution became homogeneous. This precursor solution was then calcined in a furnace at a temperature of 120 °C for 3 hours, 200 °C for 5 hours, and 400 °C for 2.5 hours, respectively. The precursors, mixed with *Ananas comosus var. queen* extract as a chelating agent, were then treated for heating at various calcination temperatures from 500 to 900 °C. On the other hand, the sample that used *Ananas comosus var. cayenne* as a chelating agent was calcined at 700 °C and 800 °C. The calcination process took 5 hours. After the whole process was finished, the samples were then characterized by Scanning Electron Microscopy (SEM) to observe the morphology formed of ZnO, and X-ray diffraction (XRD) analysis was also used to determine the crystal structure of the ZnO sample.

### *2.3. Photocatalysis analysis*

For studying the photocatalysis process, two 50 ml beaker glass with 20 ml volume of methylene blue were dissolved in 500 ml of aquadest with 10, 12, and 15 ppm concentration, respectively. After that, 100 mg of the ZnO nanostructures sample were then added to one of two beaker glasses. Both beaker glass were stored inside the black box and then irradiated with UV light. During the exposure process, the two methylene blue solutions were stirred using a magnetic stirrer. After being irradiated, the two methylene blue solutions were then put into a centrifuge, then they were deposited for 30 minutes at a speed of 3000 rpm. The concentration of methylene blue solution that was added to the ZnO nanostructures was then calculated through the color degradation that occurs within a certain time.

## 3. Result and Discussion

### *3.1. Result of ZnO Nanostructure Synthesis*

Figure 1 below shows the photograph of ZnO nanoparticles synthesized using *Ananas comosus var. Queen* calcined at 500 ℃ (Figure 1a), 600 ℃ (Figure 1b), 700 ℃ (Figure 1c), 800 ℃ (Figure 1d), and 900 ℃ (Figure 1e). It can be seen that the color of the samples was different in every sample. On the other hand, ZnO nanostructure with *Ananas comosus var. cayenne* as chelating agent sample with calcination temperatures of 700 ℃ and 800 ℃ can be seen in Figure 2.

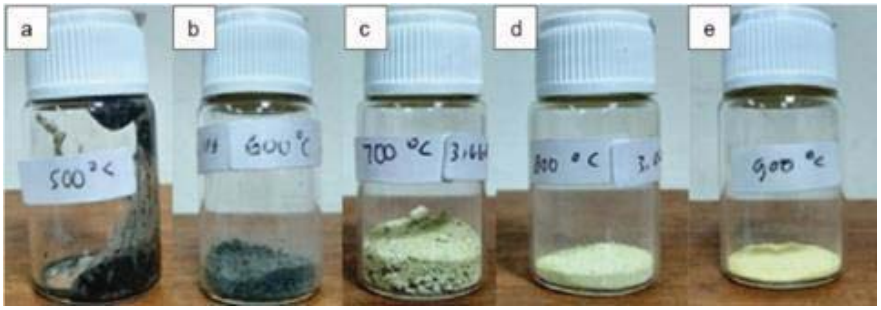


**Figure 1.** Synthesis result with different calcination temperatures using *Ananas comosus var. Queen* as a chelating agent at calcination temperatures of (a) 500 ℃, (b) 600 ℃, (c) 700 ℃, (d) 800 ℃, and (e) 900 ℃

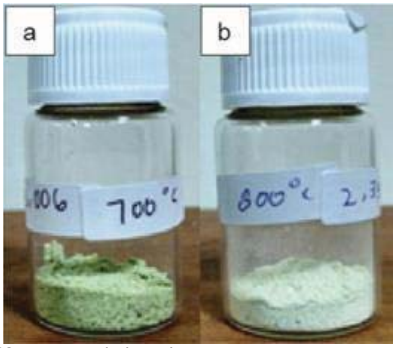


**Figure 2.** Synthesis result with different calcination temperatures using *Ananas comosus var. cayenne* (a) at 700 ℃ and (b) at 800 ℃

The temperature selection in this calcination study was based on the sugar level of each pineapple extract. The sugar level for each type of pineapple is shown in the table below.

**Table 1.** Percentage of Sugar Levels of Pineapple Extract

| Sample | %Total Sugar Level (%) | | Average |
|---|---|---|---|
| Ananas comosus var. cayenne | Repetition 1 | 40.82 | 41.305 |
| | Repetition 2 | 41.79 | |
| Ananas comosus var. Queen | Repetition 1 | 52.93 | 54.295 |
| | Repetition 2 | 55.66 | |

According to the result of the synthesis of ZnO nanostructures using *Ananas comosus var. Queen* as its chelating agent, ZnO nanostructures are still in their sol-gel form when the temperature is set to 500 ℃ (Figure 1a). Dry granules with a blackish gray color are visible when the temperature reaches 600 ℃ (Figure 1b). When the temperature reached 700 ℃, the color shifted to a greenish-white (Figure 1c). In 800 ℃ the color changed to a light green yellowish (Figure 1d), and finally white dry granules are produced when the temperature reaches 900 ℃ (Figure 1e). Meanwhile, when *Ananas comosus var. cayenne* is used as a chelating agent, the ZnO nanostructures change their form into powder at 700 ℃ and have a smoother texture at 800 ℃ (Figure 2a and b).

*3.2. Characterization of Synthesized ZnO Nanostructure*

The surface morphology of ZnO nanostructures was characterized using Scanning Electron Microscopy (SEM). The sample chosen to be studied for its morphology was a sample ZnO nanostructure synthesized with *Ananas comosus var. Queen* as its chelating agent. This is because the *Ananas comosus var. Queen* has the highest sugar level; that would be the important parameter during the sol-gel process. A sample with a calcination temperature of 800 °C was then chosen due to its brighter appearance and smoother texture. The appearance of the chosen sample can be caused by reduced particle size in the nanometer dimension [38]. The result of morphological structure can be seen in Figure 3. To determine the particle size, the software ImageJ was used. From the images, it is shown that the ZnO nanostructures formed the hexagonal shape within a size range of 0.540-3.614 μm in size and with an average of 1.858 μm. The particle size produced was still too large, possibly due to agglomeration.

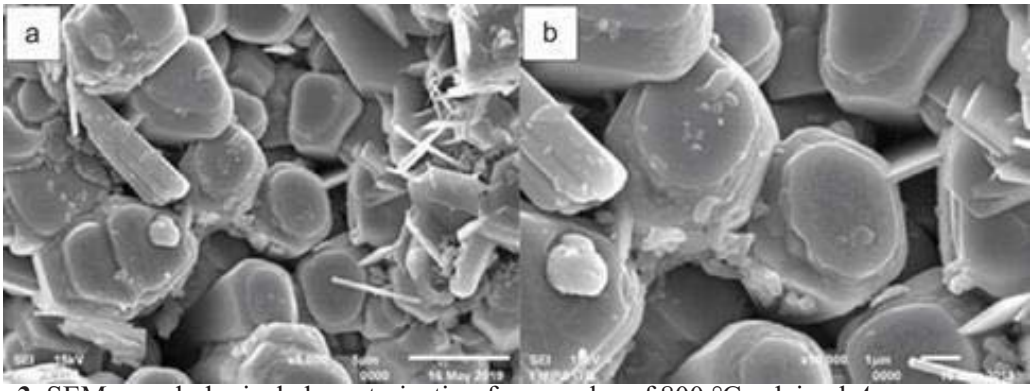


**Figure 3.** SEM morphological characterization for samples of 800 ℃ calcined *Ananas comosus var. Queen* with a) Scale of 5.000x b) Scale of 10.000x

XRD characterization was conducted to find out the crystalline structure and the crystallite size of ZnO crystals. ZnO nanostructures with calcination temperatures of 700 ℃ and 800 ℃ were chosen to be tested since it is needed to know the relationship between crystalline and their morphologies. The result was then analyzed using XRD MATCH! software and referring to the ZnO JCPDS 36-1452

database. According to the result of the XRD test in Figure 4, it can be seen that the formed spectrum has a narrow, high, and sharp peak as a result of the formation of crystals, and the ZnO nanostructures have high crystallinity properties. A sample with a calcination temperature of 700 ℃ has 31.77°, 34.38°, 36.28°, 47.56°, 56.63°, and 62.91° as its highest peak point. A sample with a calcination temperature of 800℃ has 31.79°, 34.47°, 36.29°, 47.57°, 56.60°, and 62.9° as its highest peak point.

Both samples have hexagonal shaped and wurtzite crystal structures, which have crystal parameters of a = 3.25 x $10^{-10}$ m and c = 5.21 x $10^{-10}$ m. Crystallite size can be calculated using the Scherrer equation; the average crystallite size of ZnO nanostructures with calcination temperatures of 700 ℃ is 30.90 nm, and the other sample size has a bigger size of 35.10 nm.

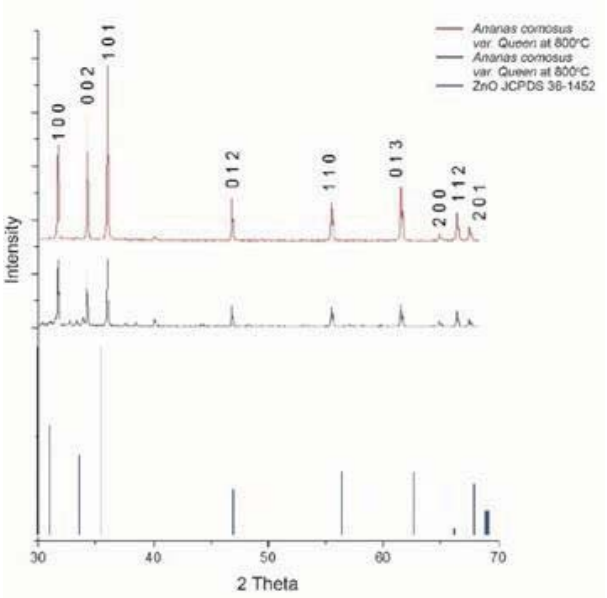


**Figure 4.** XRD patterns of ZnO nanostructures synthesized using *Ananas comosus var. Queen* as a chelating agent at a) 700 ℃ and b) 800 ℃

3.3 *Photocatalytic Activity*

ZnO nanostructures were then used for studying their photocatalytic properties. The tests were then carried out to study the effect of calcination temperature and the morphology produced on the photocatalytic properties of the ZnO nanostructures. For the first, some samples using *Ananas comosus var. Queen* as a chelating agent were applied. Calcination temperatures of 700 ℃, 800 ℃ and 900 ℃ were then studied for their photocatalytic properties. For each sample, 100 mg of ZnO nanostructures were then mixed into 20 ml of methylene blue solution with a 10, 12, and 15 ppm concentration, respectively. The solution of ZnO nanostructures and methylene blue was then exposed to UV light for 150 minutes. The results are presented in Figure 5, which shows the performance of the ZnO nanostructures with different calcination temperatures and methylene blue concentrations under the same exposure time.

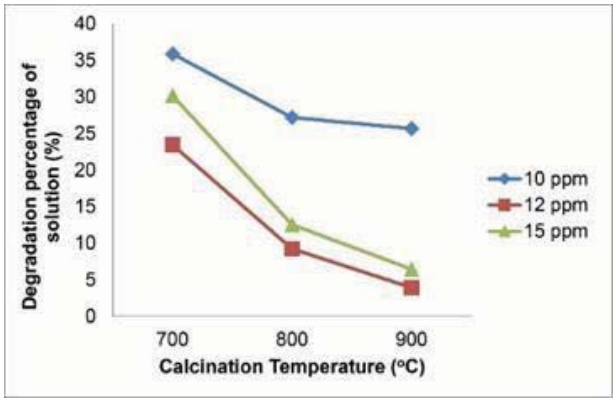


**Figure 5.** Degradation percentage and their relationship to calcination temperature ZnO nanostructures using *Ananas comosus var. Queen* as chelating agent using 100 mg sample and 150 minutes irradiation time

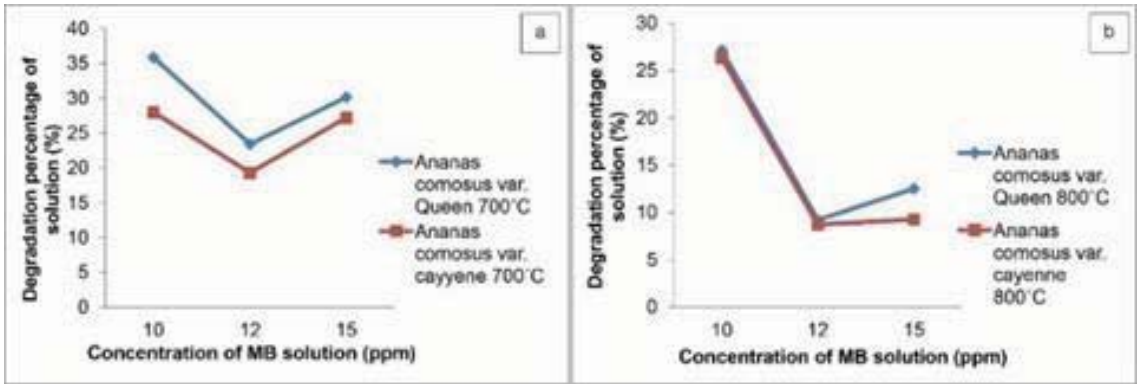


**Figure 6.** Comparison of the application of ZnO nanostructure photocatalysts using a sample of 100 mg in 150 minutes of exposure time. *Ananas comosus var. Queen* and *Ananas comosus var. cayenne* chelating agent at calcination temperature of a) 700 ℃ b) 800 ℃

The higher calcination temperature will produce ZnO nanostructures with less ability to degrade methylene blue solution. When the crystallite size of the sample is getting bigger and the surface area gets smaller, the ability to bind methylene blue will decrease, resulting in weak degradation performance. This result corresponds to an XRD result where the ZnO with a calcination temperature of 700 °C has smaller crystallite size than the other one with a calcination temperature of 800 ℃. The optimum methylene blue degradation rate is at 700 ℃ where it can degrade until 35.86% at 10 ppm methylene blue concentration. At a concentration of 12 ppm and 15 ppm, the best solution degradation rate is also in the sample with a calcination temperature of 700 ℃.

Figure 6 shows the differences between *Ananas comosus var. Queen* and *Ananas comosus var. cayenne* as chelating agents with different concentrations of methylene blue solution, which has 10, 12, and 15 ppm and an exposure time to UV light for 150 minutes. The samples using *Ananas comosus var. Queen* as a chelating agent are able to degrade better than samples using *Ananas comosus var. cayenne* as a chelating agent. This is due to the fact that the total sugar level of *Ananas comosus var. Queen* is higher than the total sugar level of *Ananas comosus var. cayenne*. The chelating agent with a higher total sugar content allows less agglomeration, so the smaller particle size was obtained. From both samples, the one with the highest degradation percentage of the methylene blue solution is the one with a calcination temperature of 700 ˚C compared to 800 ˚C. It is also known that in methylene blue with 12 ppm has 23.43% degradation percentage and 30.15% at 15 ppm. This result was not better than the degradation percentage of methylene blue with a 10 ppm concentration, which is 35.86%.

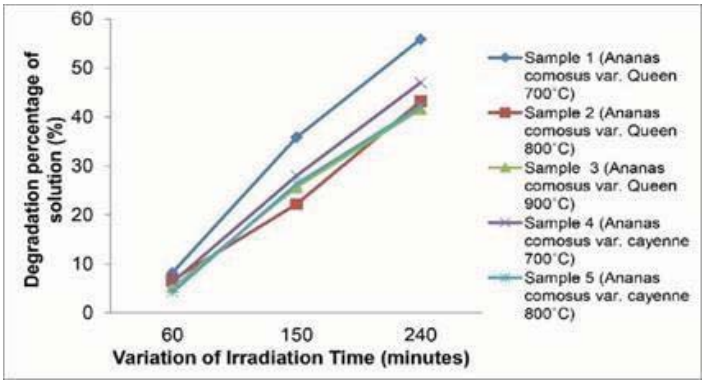


**Figure 7.** Comparison of five samples to the variation of irradiation time in the 10 ppm concentration of methylene blue solution

The longer the exposure time will make more electrons move to the conduction band and produce holes in the valence band. This causes many super hydroxides and hydroxyls to be formed, which have the function of degrading methylene blue [39]. Figure 7 shows the result of experiments conducted with 100 mg ZnO nanostructures with different chelating agents calcined at different temperatures and dissolved in a 10 ppm methylene blue solution with varying exposure times of 60, 150, and 240 minutes.

Figure 8 shows us that adding different mass variations of ZnO nanostructures chelated using *Ananas comosus var. Queen* with a 700 ºC calcination temperature to a methylene blue solution will have an effect on the degradation result with 240 minutes of exposure time. The addition of 100 mg of ZnO nanostructures had a better degradation result than the additions of 80 mg and 120 mg of nanostructures. This happens because if the 80 mg of ZnO nanostructures are added in a small amount, they will not work optimally because the electron excitation that occurs is not enough to degrade the methylene blue solution. Likewise, with the addition of 120 mg, adding too many samples will result in suboptimal exposure. This is because a large number of ZnO nanostructures will overlap and cause part of the ZnO nanostructured sample to be covered at the time of irradiation, causing saturation.

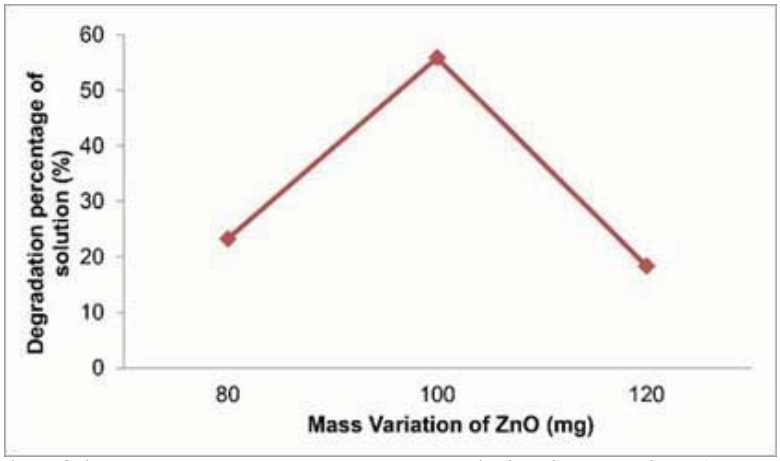


**Figure 8.** Results of the ZnO Nanostructures Mass Variation in Sample 1 (*Ananas comosus var. Queen* at 700 °C)

## 4. Conclusion

The morphology of ZnO nanostructures with *Ananas comosus var. Queen* chelating agent at calcination temperature of 800 °C shows an average particle size of 1.858 μm and an average crystalline size of 30.09 nm. ZnO with *Ananas comosus var. Queen* chelating agent at calcination temperature of 700 °C, the result shows that the crystalline size is 17.59 – 45.54 nm and averages 30.90 nm in size. Both samples have a hexagonal wurtzite crystalline structure with a = 3.25 x $10^{-10}$ m and c = 5.21 x $10^{-10}$ m. The

optimum degradation occurs in the sample with *Ananas comosus var. Queen* as the chelating agent, which has a calcination temperature of 700 °C. Within 240 minutes of irradiation, the degradation rate that occurred was 55.87% at a concentration of 10 ppm methylene blue solution.

**Acknowledgments**
The research described in this paper was financially supported by the Kementrian Pendidikan, Kebudayaan, Riset dan Teknologi Republic Indonesia, under grant number of 003/SP2H/RT-MONO/LL4/2023; 343/PNLT2/PPM/2023.

**References**
[1] C. Quay. Water Quality Impacts of the Citarum River on Jakarta and Surrounding Bandung Basin. Senior Thesis. The Ohio State University. 2018.
[2] B. Lellis, C. Z. Fávaro-Polonio, J. A. Pamphile, and J. C. Polonio. Effects of textile dyes on health and the environment and bioremediation potential of living organisms. Biotechnology Research and Innovation. 2019; **3**, 275-290.
[3] Karaghool, Haneen A. Kh. Biodecolorization of methylene blue using aspergillus, Earth and Environmental Science. 2021; 779
[4] Malik , Ahmed, et al. Investigation of textile dyeing effluent using activated sludge system to assess the removal efficiency. Water Environment Research. 2021; **93**, 2931-2940.
[5] Y.V. Nancharaiah and G.K. Kumar Reddy. Aerobic granular sludge technology: Mechanisms of granulation and biotechnological applications. Bioresour Technol. 2018; **247**, 1128-1143.
[6] Hou, Yizhi, et al. Structural Characteristics of Aerobic Granular Sludge and Factors That Influence Its Stability: A Mini Review. Wastewater Treatment and Reuse. 2021; **13**, 2726.
[7] Krishnamoorthy, Ramasamy, et al. Long-Term Exposure to Azo Dyes from Textile Wastewater Causes the Abundance of Saccharibacteria Population. Environmental Factors Shaping the Soil Microbiome. Appl. Sci. 2021; **11**, 379.
[8] T. Fazal, A. Mushtaq, F. Rehman, A. Ullah Khan, N. Rashid, W. Farooq, et al. Bioremediation of textile wastewater and successive biodiesel production using microalgae. Renew Sustain Energy Rev. 2018; **82**, 3107-3126.
[9] Fazal, Tahir , et al. Integrating bioremediation of textile wastewater with biodiesel production. Chemosphere. 2021; **281**.
[10] Lee, Qian Ying and Hong Li. Photocatalytic Degradation of Plastic Waste: A Mini Review, Recent Advances in Nanotechnology and Nanomaterials. Micromachines. 2021; **12**, 907.
[11] Mediouni, Nouha, et al. Impact of structural defects on the photocatalytic properties of ZnO. Journal of Hazardous Materials Advances. 2022.
[12] D. Štrbac, C.A Aggelopoulos, G. Štrbac, M. Dimitropoulos, M. Novaković, T. Ivetić, et al. Photocatalytic degradation of Naproxen and methylene blue: Comparison between ZnO, TiO2 and their mixture. Process Saf Environ Prot. 2018; **113**, 174-183.
[13] Ghanem , Ahmed F., et al. Synergistic effect of zinc oxide nanorods on the photocatalytic performance. Heliyon. 2020; **6**.
[14] Vignesh K, et al. Synthesis and characterization ZnO nanoparticles using sol-gel method and their antibacterial study. Materials Science and Engineering. 2022.
[15] Khanizadeh, B., Khosravi, M., Behnajady, M. A., Shamel, A., & Vahid, B. Mg and La. Co-doped ZnO nanoparticles prepared by sol–gel method: synthesis, characterization and photocatalytic activity. Periodica Polytechnica Chemical Engineering. 2020; **64**, 61-74.
[16] Bhardwaj, R., Bharti, A., Singh, J. P., Chae, K. H., Goyal, N., & Gautam, S. Structural and electronic investigation of ZnO nanostructures synthesized under different environments. Heliyon. 2018; **4**, e00594.
[17] Al-Bataineh, Q. M., Alsaad, A. M., Ahmad, A. A., & Al-Sawalmih, A. Structural, electronic and optical characterization of ZnO thin film-seeded platforms for ZnO nanostructures: sol–gel method versus ab initio calculations. Journal of Electronic Materials. 2019; **48**, 5028-5038.

[18] Elfaham, Mohamed M., Mostafa, Ayman M., Mwafy, Eman A. The effect of reaction temperature on structural, optical and electrical properties of tunable ZnO nanoparticles synthesized by hydrothermal method. Journal of Physics and Chemistry of Solids. 2021; **154**, 110089.
[19] Bazazi, S., Arsalani, N., Khataee, A., & Tabrizi, A. G. Comparison of ball milling-hydrothermal and hydrothermal methods for synthesis of ZnO nanostructures and evaluation of their photocatalytic performance. Journal of industrial and engineering chemistry. 2018; **62**, 265-272.
[20] Faisal, M., Harraz, F. A., Jalalah, M., Alsaiari, M., Al-Sayari, S. A., & Al-Assiri, M. S. Polythiophene doped ZnO nanostructures synthesized by modified sol-gel and oxidative polymerization for efficient photodegradation of methylene blue and gemifloxacin antibiotic. Materials Today Communications. 2020; **24**, 101048.
[21] Iqbal, M., Thebo, A. A., Jatoi, W. B., Tabassum, M. T., Rehman, M. U., Thebo, K. H., ... & Shah, I. Facile synthesis of Cr doped hierarchical ZnO nano-structures for enhanced photovoltaic performance. Inorganic Chemistry Communications. 2020; **116**, 107902.
[22] J. Wojnarowicz, T. Chudoba, I. Koltsov, S. Gierlotka, S. Dworakowska and W. Lojkowski. Size control mechanism of ZnO nanoparticles obtained in microwave solvothermal synthesis. Nanotechnology. 2018; **29**, 065601.
[23] Pineda-Reyes, Ana M. and M. de la L. Olvera. Synthesis of ZnO nanoparticles from water-in-oil (w/o) microemulsions. Materials Chemistry and Physics. 2018; **203**, 141-147.
[24] Mousavi, Seyyed Mojtaba, et al. Shape-controlled synthesis of zinc nanostructures mediating macromolecules for biomedical applications. Biomaterials Research. 2022; **26.1**, 1-20.
[25] Liang, Yucang, et al. Organozinc Precursor-Derived Crystalline ZnO Nanoparticles: Synthesis, Characterization and Their Spectroscopic Properties. Nanomaterials. 2018; **8**, 22.
[26] A. Henni, N. Harfouche, A. Karar, D. Zerrouki, F.X. Perrin and F. Rosei. Synthesis of graphene–ZnO nanocomposites by a one-step electrochemical deposition for efficient photocatalytic degradation of organic pollutant. Solid State Sci. 2019; **98**, 106039.
[27] Kuzmin, Alexei, et al. Microwave-assisted synthesis and characterization of undoped and manganese doped zinc sulfide nanoparticles. Materials Chemistry and Physics. 2022; **290**.
[28] N. Pauzi, N. Mat Zain and N.A. Ahmad Yusof. Microwave-Assisted Synthesis for Environmentally ZnO Nanoparticle Synthesis. Springer, Singapore. 2019.
[29] Biron, Dionisio da Silva, Venina dos Santos and Carlos Pérez Bergmann. Synthesis and Characterization of Zinc Oxide Obtained by Combining Zinc Nitrate with Sodium Hydroxide in Polyol Medium. Materials Research. 2020; **23**.
[30] P.P. Mahamuni, P.M. Patil, M.J. Dhanavade, M.V Badiger, P.G. Shadija, A.C Lokhande, et al. Synthesis and characterization of zinc oxide nanoparticles by using polyol chemistry for their antimicrobial and antibiofilm activity. Biochem Biophys Reports. 2019; **17**, 71–80.
[31] Vijay, Aditi, et al. Understanding the role of ionic flux on the polarity of the exposed surfaces of ZnO, Physical Chemistry Chemical Physics. 2020.
[32] Blachowicz, Tomasz and Andrea Ehrmann. Recent developments in electrospun ZnO nanofibers: A short review. Journal of Engineered Fibers and Fabrics. 2020.
[33] Chen , Mingyi , et al. Nanofiber template induced preparation of ZnO nanocrystal and its application in photocatalysis. Scientific Reports. 2021.
[34] Sugihartono, I, D Dianisya and I Isnaeni. Crystal structure analyses of ZnO nanoparticles growth by simple wet chemical method. Materials Science and Engineering. 2018.
[35] Jiang, Tengfei, et al. Wet chemical epitaxial growth of a cactus-like CuFeO2/ZnO heterojunction for improved photocatalysis. Dalton Transactions. 2020; **28**.
[36] S. Liu, C. Ma, M-G. Ma and F. Xu. Magnetic Nanocomposite Adsorbents. Composite Nanoadsorbents. Elsevier. 2019.
[37] R.A. Raja Ahmad, Z. Harun, M.H.D. Othman, H. Basri, M.Z. Yunos, A. Ahmad, et al. Biosynthesis of zinc oxide nanoparticles by using fruits extracts of Ananas Comosus and its antibacterial activity. Malaysian J Fundam Appl Sci. 2019; **15**, 268-273.

[38] F. Kazemi, F. Arianpour, M. Taheri, A. Saberi and H.R. Rezaie. Effects of chelating agents on the sol-gel synthesis of nano-zirconia: Comparison of the Pechini and sugar-based methods. Int J Miner Metall Mater. 2020; **27**, 693-702.
[39] C.B. Ong, L.Y. Ng and A.W. Mohammad. A review of ZnO nanoparticles as solar photocatalysts: Synthesis, mechanisms and applications. Renew Sustain Energy Rev. 2018; **81**, 536-551.